



Single/synchronous adsorption of Cu(II), Cd(II) and Cr(VI) in water by layered double hydroxides doped with different divalent metals

Xiao-tong Chen^a, Xing-peng Liu^b, Hui-qiang Li^{a,*}, Di Bao^a, Ping Yang^a

^aCollege of Architecture and Environment, Sichuan University, Chengdu 610065, China, Tel. +8618980668020; email: lhq_scu@163.com (H.-q. Li), Tel. +8613032872057; email: 1137129848@qq.com (X.-t. Chen), Tel. +8618225600405; email: baodi33@126.com (D. Bao), Tel. +8618602804508; email: yping63@163.com (P. Yang)

^bCollege of Communication Engineering, Chengdu Technological University, Chengdu 611730, China, Tel. +8618980669653; email: lxp_herb@163.com (X.-p. Liu)

Received 1 December 2021; Accepted 13 May 2022

ABSTRACT

Layered double hydroxides (LDHs) are a class of excellent adsorbents for the simultaneous removal of anionic and cationic pollutants in water. In this paper, four types of LDHs doped with different divalent metals were prepared by the co-precipitation method, namely MgAl-LDH, ZnAl-LDH, CaAl-LDH and CoAl-LDH, to explore their adsorption performance for Cu(II), Cd(II) and Cr(VI) respectively. The removal efficiencies of Cu(II) and Cd(II) by MgAl-LDH and CaAl-LDH were higher, and the removal efficiencies of Cr(VI) by MgAl-LDH and CoAl-LDH were higher. In comparison, MgAl-LDH showed the best all-around adsorption performance, and its corresponding optimal dosage was 0.50 g/L. Effects of pH, initial pollutant concentration, coexisting heavy metals and coexisting anions on adsorption by MgAl-LDH were studied. The adsorption behavior of MgAl-LDH was consistent with the pseudo-second-order kinetic model and the Freundlich isotherm model. In the synchronous adsorption system, the removal efficiencies of MgAl-LDH for Cu(II), Cd(II) and Cr(VI) reached 99.50%, 70.28% and 22.50%, respectively. Combined with scanning electron microscopy, energy-dispersive X-ray spectroscopy, Fourier-transform infrared spectroscopy, X-ray diffraction and Brunauer–Emmett–Teller characterization results, the main removal mechanisms of Cu(II), Cd(II) and Cr(VI) were deduced.

Keywords: Single adsorption; Synchronous adsorption; Layered double hydroxides; Heavy metals

1. Introduction

Heavy metals will persist after entering the ecosystem and are challenging to be biodegraded. Under the biological amplification of the food chain, heavy metals can be enriched thousands of times, seriously damaging the ecosystem and endangering human health [1]. According to the US Environmental Protection Agency, the most toxic heavy metals include As, Cu, Hg, Ni, Cd, Pb and Cr [2]. To remove toxic and harmful heavy metals in wastewater, chemical precipitation, evaporation, oxidation, ion

exchange, membrane filtration, solvent extraction, coagulation–flocculation, flotation, electrochemical treatment and adsorption have been developed [3,4]. Among them, adsorption is currently considered the most promising method for heavy metal wastewater treatment. Heavy metals coexisting in wastewater may interact to affect the corresponding adsorption capacity and behavior, especially for coexisting cations and anions [5]. For most adsorbents, it is difficult to simultaneously eliminate heavy metals in anionic and cationic states from water. For example, using surfactants to organically modify kaolin and

* Corresponding author.

then conducting electrostatic adsorption through surface organic functional groups is a method to remove heavy metal anions from wastewater. Still, the adsorption performance of this method for cations is not ideal [6]. The activated carbon adsorption process can effectively remove cationic heavy metals such as Hg^{2+} [7], but cannot effectively remove oxyanion metals such as As, Cr and Se [8,9]. Therefore, there is an urgent need to design and prepare a green adsorbent material with low cost, easy synthesis, good adsorption performance and easy recycling.

The general structural formula of layered double hydroxides (LDHs) is $[\text{M}_{1-x}^{2+}\text{M}_x^{3+}(\text{OH})_2]^{x+}[\text{A}^{n-}]_{x/n} \cdot y\text{H}_2\text{O}$, where M^{2+} and M^{3+} represent divalent and trivalent metal cations respectively, and A^{n-} represents interlayer n -valent anions. The interlayer also contains water molecules [10]. The value of x is equal to the molar ratio of $\text{M}^{3+}/(\text{M}^{2+} + \text{M}^{3+})$, usually in the range of $0.18 < x < 0.33$ [11]. The types of M^{2+} and M^{3+} would affect the unit cell parameters, following a change of interlayer spacing such as spatial symmetry or spacing distance. The change of the x value affects the purity of LDHs, and the distance between M^{2+} and M^{3+} causes a change in the layer charge density. These features will eventually impact the molecular mechanism between the hydroxide layer and the interlayer anion [12]. The laminates of LDHs have the brucite-type regular octahedral structure [13], so MgAl-LDH is the most common and basic LDH material. It is generally believed that M^{2+} and M^{3+} can covalently bond with the $-\text{OH}$ groups in the laminates to form LDHs as long as the radii of the metal cations in the laminates are not much different from that of Mg^{2+} [14]. Therefore, the types and proportions of M^{2+} and M^{3+} on the layers of LDHs can be freely adjusted according to actual needs.

LDHs are excellent adsorbent materials for the treatment of heavy metal wastewater, and changing the composition of metals can enhance the adsorption effect of LDHs on specific pollutants. Zhang et al. [15] synthesized a novel sodium alginate intercalated MgAl-LDH, and the maximum adsorption capacities of the material for Cu(II), Pb(II) and Cd(II) reached 0.945, 1.176 and 0.850 mmol/g, respectively. Azad and Mohsennia [16] prepared a novel polyvinyl butyral-polyacrylonitrile/ZnAl-LDH nanocomposite membrane, and the simultaneous removal of Pb^{2+} and Cd^{2+} were the highest at pH 5 and 6, reaching 97.76% and 87.63%, respectively. Wang et al. [17] synthesized LDH materials composed of Mg/Al, Ni/Al and Zn/Al with a molar ratio of $\text{M}^{2+}/\text{Al}^{3+} = 3$, and ZnAl-LDH exhibited excellent adsorption capacity (68.07 mg/g) and good regeneration performance for Cr(VI). Kameda et al. [18] prepared NiAl-LDH and CoAl-LDH and found that they removed Cr(VI) mainly by anion exchange of $\text{Cr}_2\text{O}_7^{2-}$. The maximum adsorption capacity and equilibrium adsorption constant values were 2.0 mmol/g and 2.4 for NiAl-LDH, and 1.9 mmol/g and 1.5 for CoAl-LDH, respectively. There were also some research reports on the synchronous adsorption of various heavy metal anionic and cationic pollutants by LDHs. For example, Yue et al. [19] prepared Mg-Al-Cl layered dihydroxides (Cl-LDH). They found that the adsorption of coexisting Cu(II) and Cr(VI) by Cl-LDH promoted the removal of Cu(II) while did not affect the adsorption of Cr(VI) in low concentrations (≤ 40 mg/L). Milagres et al. [20] found that CaAl-LDH with a $\text{Ca}^{2+}/\text{Al}^{3+}$ molar ratio of 4:1 (4HC) could

simultaneously remove 90%, 50% and 50% of Cu^{2+} , Ni^{2+} and Zn^{2+} (200 mg/L). The amount of metal removed followed the order of magnitude of its hydroxyl complex formation constant. 4HC could also remove 60%, 57% and 52% of Cr(VI) (200 mg/L) while completely removing Cu^{2+} , Ni^{2+} or Zn^{2+} (400 mg/L), respectively.

In this study, we prepared four LDH materials (MgAl-LDH, ZnAl-LDH, CaAl-LDH and CoAl-LDH) by the same method, and compared the single/synchronous adsorption performance of these materials for Cu(II), Cd(II) and Cr(VI) under the same experimental conditions. Then the use parameters of the optimal adsorbent material were further optimized, and the adsorption mechanisms were proposed. Our study aims to provide help for optimizing the composition of LDH adsorbents and simultaneously removing heavy metal anionic and cationic pollutants in wastewater.

2. Materials and experiments

2.1. Reagents

Potassium dichromate ($\text{K}_2\text{Cr}_2\text{O}_7$), copper chloride ($\text{CuCl}_2 \cdot 2\text{H}_2\text{O}$), cadmium chloride ($\text{CdCl}_2 \cdot 2.5\text{H}_2\text{O}$), hydrochloric acid, phosphoric acid, sulfuric acid, sodium hydroxide (NaOH), sodium carbonate (Na_2CO_3), magnesium chloride ($\text{MgCl}_2 \cdot 6\text{H}_2\text{O}$), zinc chloride ($\text{ZnCl}_2 \cdot 6\text{H}_2\text{O}$), cobalt chloride ($\text{CoCl}_2 \cdot 6\text{H}_2\text{O}$), calcium chloride (CaCl_2), aluminum trichloride ($\text{AlCl}_3 \cdot 6\text{H}_2\text{O}$), sodium alginate, acetone ($\text{C}_3\text{H}_6\text{O}$), polyethylenimine (PEI, M.W.600, 99%), glutaric dialdehyde ($\text{C}_5\text{H}_8\text{O}_2$, 50%) and absolute ethanol ($\text{C}_2\text{H}_6\text{O}$) were obtained from Kelong Chemical Reagent Co., Ltd., (Chengdu, Sichuan, China). Diphenylcarbazine ($\text{C}_{13}\text{H}_{14}\text{N}_4\text{O}$) was purchased from Meilun Bio. All the above chemical reagents were of analytical grade without further purification.

2.2. Preparation of LDH materials

The adsorption materials used in this experiment were synthesized by the co-precipitation method. Taking magnesium-aluminum hydroxide (MgAl-LDH) as an example, the main steps were as follows: firstly, 0.15 mol of magnesium chloride and 0.05 mol of aluminum chloride were respectively weighed, and dissolved in 100 mL of deionized water, and stirred until fully dissolved to form a homogeneous salt solution, in which the molar ratio of metal ions was $n(\text{M}^{2+}):n(\text{M}^{3+}) = 3:1$. Then, 0.3 mol of sodium hydroxide and 0.1 mol of sodium carbonate were dissolved in 100 mL of deionized water and stirred evenly to obtain an alkali solution. After that, the mixed salt solution was dropped into a 500 mL conical flask at a uniform efficiency, and then the alkali solution was slowly added. The pH value of the mixed solution was kept at about 10 by controlling the drop acceleration of the alkali solution. The mixed solution was continuously stirred by magnetic force for 1 h at room temperature (25°C) to make it thoroughly mixed. Finally, the aged solution was centrifuged at 3,000 r/min for centrifugation separation. The resulting product was thoroughly washed with deionized water to neutral, dried at 65°C for 24 h, ground, and crushed with a ceramic mortar. Then the white powdered MgAl-LDH material was obtained after a 200 mesh sieve.

By changing the kinds of heavy metal ions on the layer, three other types of LDH materials (ZnAl-LDH, CaAl-LDH and CoAl-LDH) were prepared. The preparation methods and conditions were consistent with those of MgAl-LDH material.

2.3. Sample characterization

Morphological and elemental analysis of the samples was characterized by scanning electron microscope and energy-dispersive X-ray spectroscopy (SEM-EDS, JSM-7500F, Japan). Fourier-transform infrared spectroscopy (FTIR, Nicolet 5700, United States, measurement range: 4,000–400 cm^{-1}) was used to determine the chemical structure of materials or confirm the chemical groups contained in them. The crystal structures of the composites were monitored with X-ray diffraction (XRD, Empyrean, Netherlands, scanning range: 5°–90°). Brunauer–Emmett–Teller measurements were performed to characterize the specific surface area, by using an ASAP 2460 surface area analyzer from Micromeritics (The United States).

2.4. Adsorption experiments

The following solutions were prepared: (a) 10 mg/L Cu(II) solution, (b) 10 mg/L Cd(II) solution, (c) 10 mg/L Cr(VI) solution, (d) Cu(II), Cd(II) and Cr(VI) each 10 mg/L mixed solution. 0.025, 0.05, 0.075 and 0.10 g of adsorbents were added to 100 mL of the above solutions with continuous stirring over a magnetic stirrer at 200 rpm. The reaction temperature was maintained at $25^\circ\text{C} \pm 1^\circ\text{C}$. 0.1 mol/L of HCl and 0.1 mol/L of NaOH were used to adjust the initial pH. The concentration range of the heavy metal solutions was: Cu(II) (10–150 mg/L), Cd(II) (10–100 mg/L), Cr(VI) (5–30 mg/L). When exploring the influence of coexisting metal ions, the initial concentration of one heavy metal ion increased, and the other two were kept at 10 mg/L. After the reactions, the aqueous solution was filtered by a 0.45 μm membrane. The filtrate was used to determine concentrations of Cu(II), Cd(II) (using flame atomic absorption spectrophotometry) and Cr(VI) (using diphenylcarbazide spectrophotometric method (GB 7467-87)). Each experiment was done in three parallel groups.

The formulas for removal efficiency (%) and adsorption capacity (mg/g) are as follows:

$$\text{Removal efficiency } R = \frac{C_0 - C_t}{C_0} \times 100 \quad (1)$$

$$\text{Adsorption capacity } q_e = \frac{(C_0 - C_t)V}{m} \quad (2)$$

where C_0 and C_t (mg/L) are the initial concentration and the concentration at time t of heavy metal ions, respectively; V (L) is reaction solution volume; m (g) is adsorbent dosage.

3. Results and discussion

3.1. Optimal LDH material and dosage

The results of the single adsorption experiment are shown in Fig. 1. The removal efficiencies of Cu(II) and

Cd(II) by MgAl-LDH and CaAl-LDH were significantly higher than that of ZnAl-LDH and CoAl-LDH. The removal efficiencies of MgAl-LDH and CoAl-LDH for Cr(VI) were relatively high. The removal efficiency of CaAl-LDH on Cr(VI) was significantly lower than that of the other three adsorbents. The results of the synchronous adsorption experiment are shown in Fig. 2. The four adsorbents all showed the characteristic of preferentially adsorbing Cu(II), because the reaction between Cu^{2+} and the hydroxyl groups in LDHs had a greater stability constant, which led to rapid surface adsorption, and Cu^{2+} precipitated on LDHs, making it difficult for other metals to reach the adsorption sites [21]. In synchronous adsorption, the order of the removal efficiencies of the four LDHs to Cd(II) was: MgAl-LDH > CaAl-LDH > CoAl-LDH > ZnAl-LDH. CoAl-LDH showed the highest removal efficiency for Cr(VI), followed by MgAl-LDH. The stability and composition characteristics of adsorbents have significant influences on the adsorption effect. The stabilities of 2Mg-Al and 2Zn-Al clusters were stronger than that of 2Ca-Al clusters. Experimentally, Co^{2+} was also difficult to be introduced into LDH layers as the only divalent component because the large octahedral CFSE of low spin d_6 configuration of Co^{3+} facilitated the easy oxidation of Co^{2+} to Co^{3+} . The cluster including Mg^{2+} showed a stronger Lewis-type bond than the cluster including Zn^{2+} [22]. Therefore, MgAl-LDH was the easiest to be synthesized and the most stable. Besides, the acid-base properties of LDHs mainly came from M(II)O-H . With the increase of the divalent metal ion radius of the laminates, the length of the M(II)O-H bond, the acidity of the laminates and the H reactivity of the O-H of the laminates increased. In this experiment, the order of the divalent ion radius on the LDH laminates was $\text{Mg}^{2+} < \text{Zn}^{2+} < \text{Co}^{2+} < \text{Ca}^{2+}$. Therefore, MgAl-LDH had the weakest acidity, which was favorable for removing Cu^{2+} and Cd^{2+} by precipitation. In CaAl-LDH, Cu(II) and Cd(II) tended to exchange with hydroxyl hydrogen at the edge of the layered structure of CaAl-LDH and were adsorbed on the surface of CaAl-LDH in the form of surface complexation. After the interlayer anion and the hydroxyl group of the laminate formed hydrogen bonds, the O_{anion} of the anion was the electron donor, and the hydroxyl group H was the electron acceptor. Among the four LDH materials, the weak acidity of OH on the MgAl-LDH laminates made the density of the interlayer anion O_{anion} the highest, the hydrogen bond was the strongest, and the layered structure MgAl-LDH- CrO_4 was the most stable, which was conducive to the adsorption of Cr(VI) by MgAl-LDH. The Mulliken charge of MgAl-LDH, CoAl-LDH and ZnAl-LDH laminate metals measured by Li were 2.7312, 2.9942 and 2.7206, respectively. The greater the Mulliken charge of the laminates, the stronger the electrostatic attraction between the laminates and the interlayer anions, so the removal efficiency of Cr(VI) by CoAl-LDH was relatively high [23]. To sum up, MgAl-LDH was more suitable as the primary material for subsequent adsorption research.

Let's discuss the optimal dosage of MgAl-LDH below. As shown in Fig. 1, the removal efficiencies of heavy metal ions gradually increased with the increase of adsorbent dosage in the single adsorption process, since the

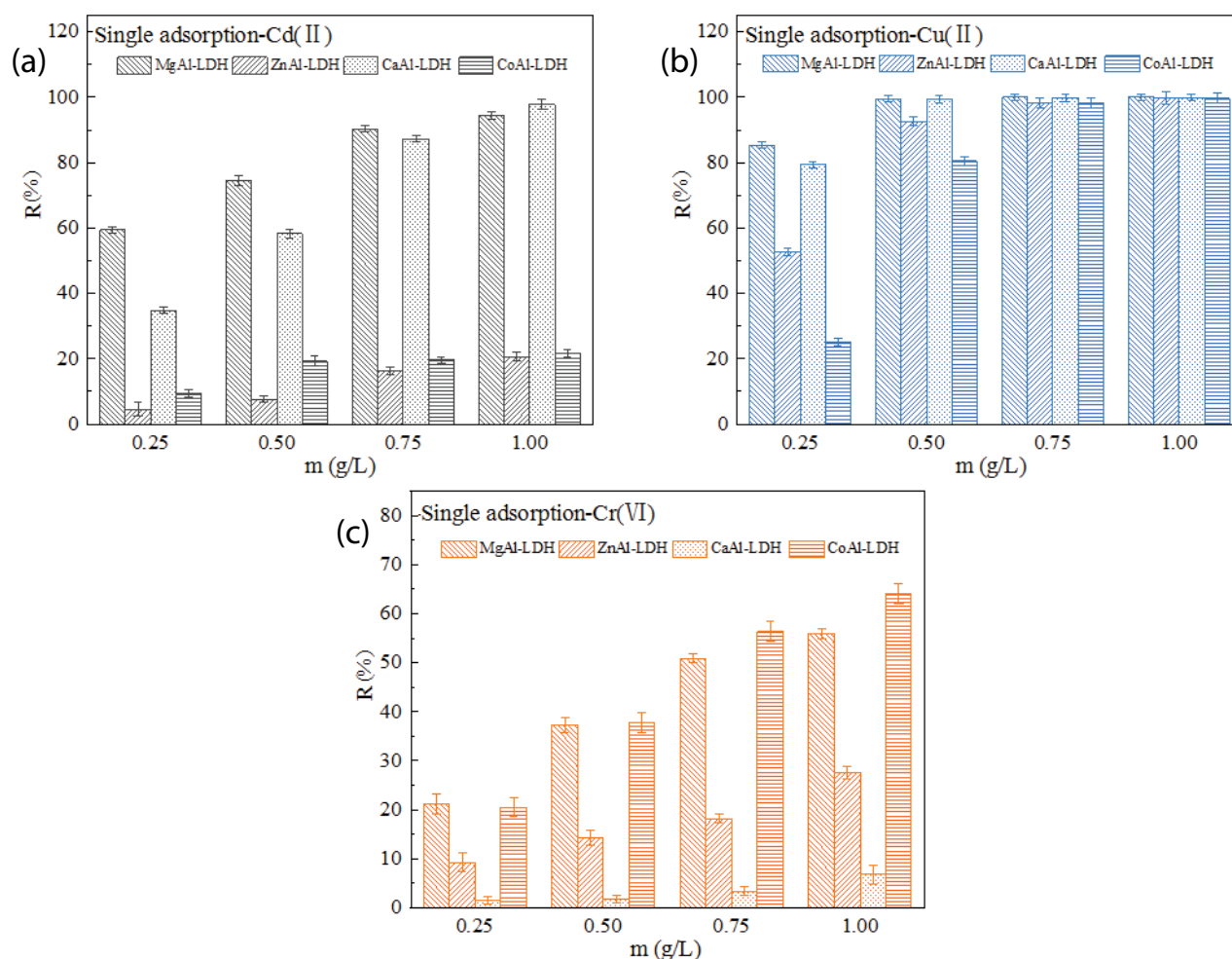


Fig. 1. Removal efficiencies of (a) Cd(II), (b) Cu(II) and (c) Cr(VI) by four LDH materials in single adsorption systems (Reaction temperature = 25°C; initial pH = 4; C_0 = 10 mg/L; V = 100 mL; stirring speed = 200 rpm).

enhancement of adsorbent dosage increased the number of adsorbable active sites [24]. After the dosage of MgAl-LDH reached 0.50 g/L, the removal efficiency of Cu(II) was close to 100% and there was no significant change, and the increasing trend of the removal efficiencies of Cd(II) and Cr(VI) slowed down. The results might be due to the formation of adsorbent clumps that reduced the available surface area and blocked some adsorption sites [25]. In the synchronous adsorption system (Fig. 2), the removal efficiency of Cu(II) by MgAl-LDH was always close to 100%. When the dosage was 0.25 g/L, the adsorption of Cd(II) was inhibited. However, compared with the single adsorption system, when the dosage of MgAl-LDH was 0.50 g/L, the removal efficiency of Cd(II) in the synchronous adsorption system dropped only by 5%. The adsorption of Cr(VI) was suppressed, which might be because the increased Cl⁻ in the synchronous adsorption system promoted the shielding of the electrostatic attraction between chromate and MgAl-LDH, and competed with chromate for surface adsorption sites [26]. Considering that the adsorption of Cd(II) and Cr(VI) was inhibited to different degrees under different dosages in the synchronous adsorption system, 0.50 g/L

was selected as the dosage of MgAl-LDH for subsequent studies to ensure a better adsorption effect.

3.2. Adsorption influencing factors

3.2.1. Initial pH

The pH dependence of metal adsorption is largely related to metal chemistry in the solution and the properties of adsorbents [27]. As shown in Figs. 3 and 4, when pH = 2, the adsorption capacities of MgAl-LDH for Cu(II) and Cd(II) were very low. With the increase in pH value, the adsorption capacities increased rapidly, and then the rate of growth slowed down. When pH = 6, the removal efficiencies of Cd(II) and Cu(II) by MgAl-LDH reached 90.29% and close to 100%, respectively. Similar conclusions were obtained in the adsorption experiments of activated carbon and kaolin for Cu(II) [28]. At a lower pH value, the surface of the adsorbents was positively charged due to protonation, and electrostatic repulsion prevented the electrostatic adsorption of Cu²⁺ and Cd²⁺ [29]. It might be possible that part of the structure of MgAl-LDH dissolved.

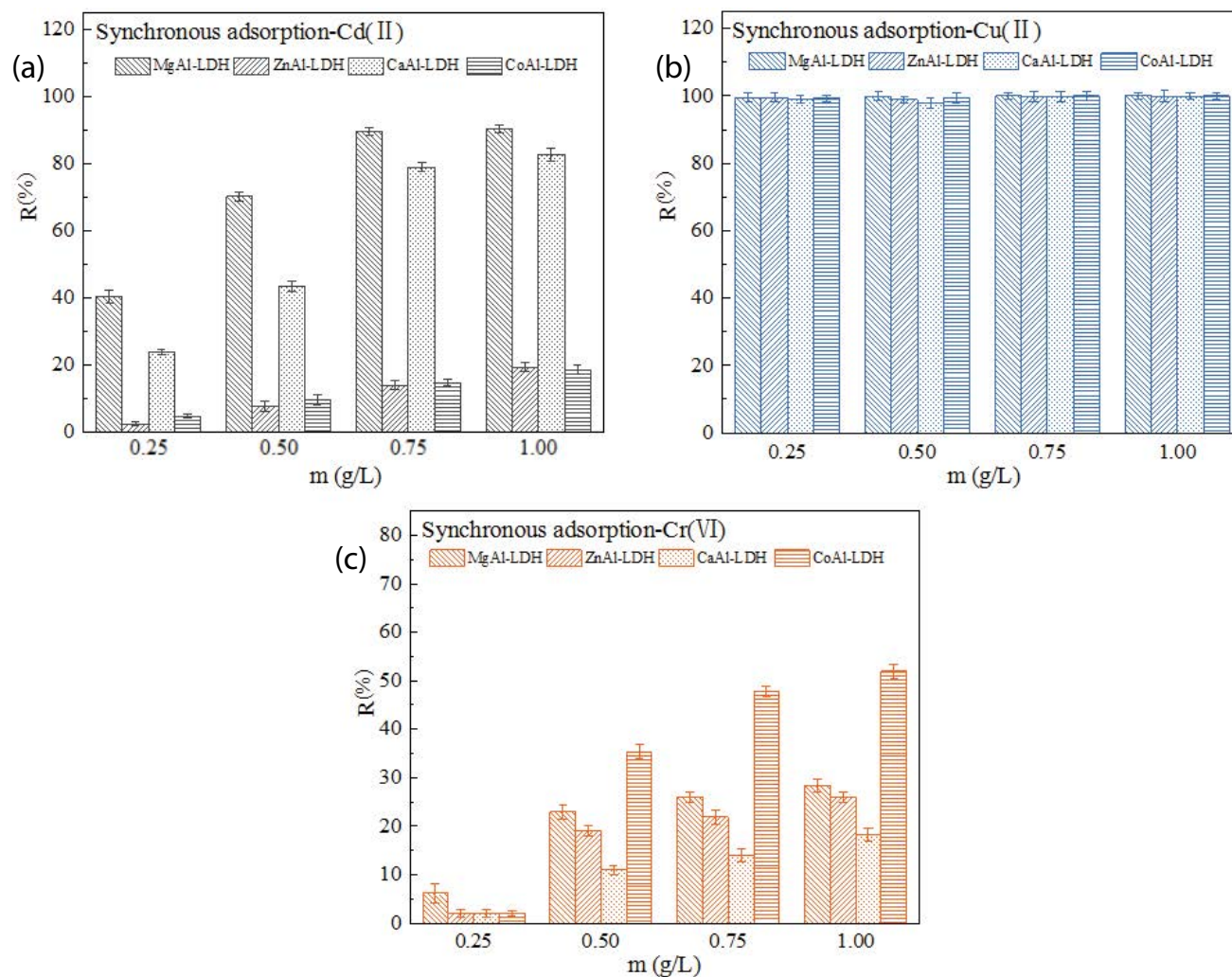


Fig. 2. Removal efficiencies of (a) Cd(II), (b) Cu(II) and (c) Cr(VI) by four LDH materials in the synchronous adsorption system (Reaction temperature = 25°C; initial pH = 4; $C_0 = 10$ mg/L; $V = 100$ mL; stirring speed = 200 rpm).

The study by Li et al. using MgAl-LDH to remove Cr(VI) also appeared in the dissolution of the adsorbent [30]. The higher the pH value, the faster the adsorption equilibrium of Cu(II) and Cd(II) on MgAl-LDH reached. In contrast to metal cations, low pH was better for the adsorption of metal oxide anions than high pH [31]. With the increase of pH, the adsorption capacity of Cr(VI) on MgAl-LDH first increased and then decreased, finally reaching stability. There was a similar trend in the research of Shi et al. [32]. When the solution was strong acidic ($\text{pH} < 2$), Cr(VI) existed in the form of electrically neutral H_2CrO_4 , which was not conducive to adsorption. When $2 < \text{pH} < 3$, Cr(VI) was mainly in the form of HCrO_4^- and a small quantity of $\text{Cr}_2\text{O}_7^{2-}$. HCrO_4^- was a negative monovalent ion. When interacting with adsorbents, HCrO_4^- required the least adsorption-free energy and occupied the fewest active sites [33]. When $\text{pH} > 3$, HCrO_4^- rapidly transformed into CrO_4^{2-} with increasing pH. As a negative divalent ion, CrO_4^{2-} required more adsorption-free energy and occupied more active sites than HCrO_4^- [34].

In Fig. 5, in the synchronous adsorption, the removal efficiency of MgAl-LDH for the three pollutants was $\text{Cu(II)} > \text{Cd(II)} > \text{Cr(VI)}$ in turn. When $\text{pH} \geq 4$, Cr(VI) showed obvious desorption after 50 min of reaction. Ling et al. found a similar desorption phenomenon in the adsorption of Cr(VI) with CoFe-LDH (initial concentration was 10 mg/L) [35], as part of Cr(VI) would enter the interlayer and be removed by ion exchange with the anions in the MgAl-LDH interlayer (CO_3^{2-} and Cl^-), which made a certain amount of CO_3^{2-} and Cl^- exist in the solution. As the reaction progressed, the Cr(VI) that entered the interlayer might be exchanged again by the anions in the solution, causing the phenomenon of desorption [36].

The equilibrium pH values were all higher than the initial pH, which might be due to the protonation and/or the dissolution of LDHs. The equilibrium pH was finally stable in 6–8, indicating that the layered hydroxides had a certain buffering effect. When Laipan et al. [37] studied the removal performance of Mg/Al-CLDH on individual heavy metal cations in single cation systems, they also

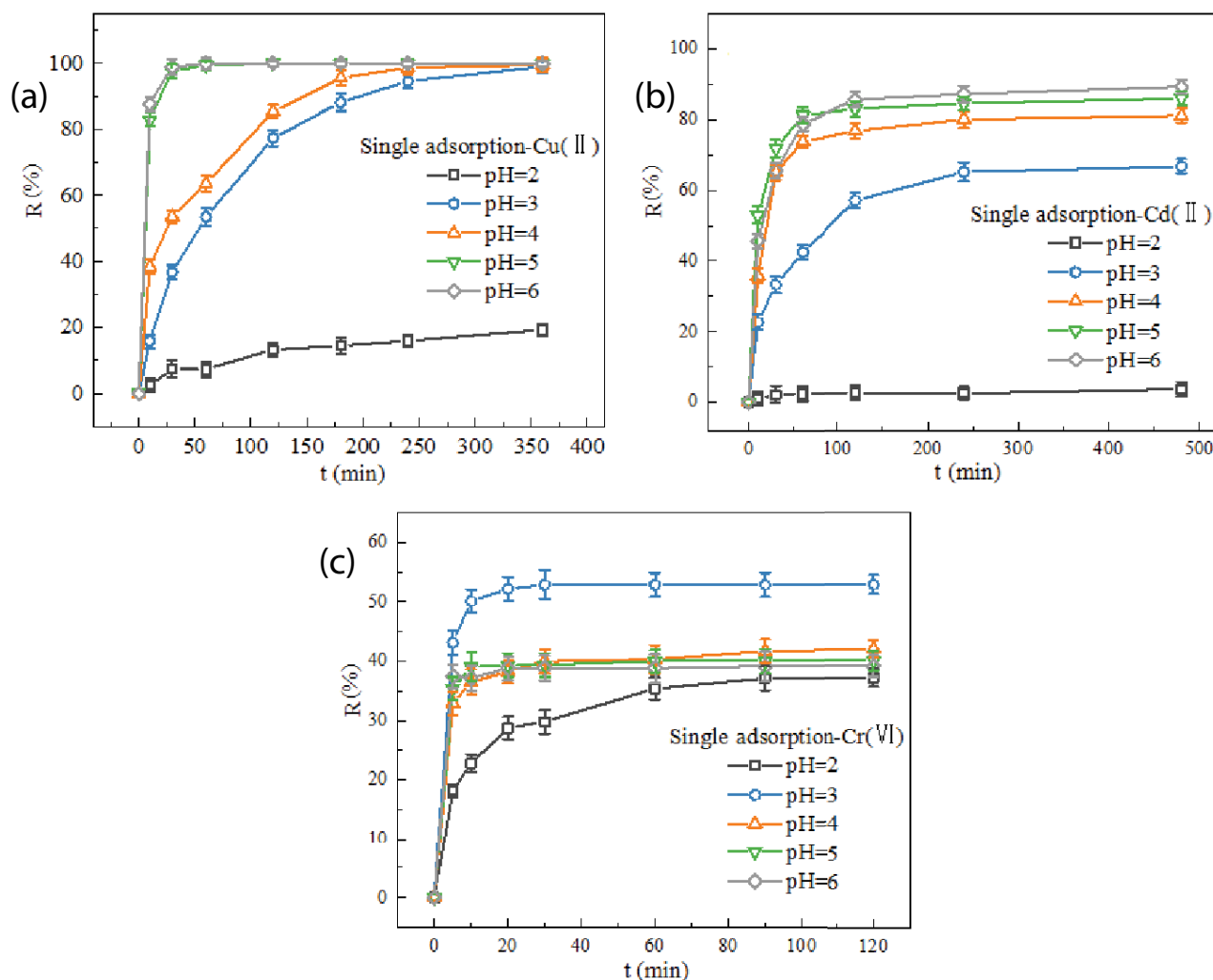


Fig. 3. Effect of initial pH value on the removal efficiencies of (a) Cu(II), (b) Cd(II) and (c) Cr(VI) in single adsorption systems (Reaction temperature = 25°C; $m = 0.50$ g/L; $C_0 = 10$ mg/L; $V = 100$ mL).

found that Mg/Al-CLDH exhibited high pH neutralization properties. In this experiment, Cu^{2+} and Cd^{2+} began hydrolytic precipitation at pH values of about 6.3 and 9.2, respectively. Kameda et al. [38] used Mg-Al-EDTA LDH to adsorb Cu^{2+} and Cd^{2+} . They adjusted and maintained the pH of the solution at 5.0 to prevent hydrolysis precipitation of Cu^{2+} and Cd^{2+} . Considering the effects of pH on the removal efficiencies of Cu(II), Cd(II) and Cr(VI) in the single/synchronous adsorption systems, and to prevent the formation of hydroxyl precipitates of Cu^{2+} and Cd^{2+} in the reaction process, the following experiments were carried out with an initial pH of 4.

3.2.2. Initial pollutant concentration

Results of the single adsorption experiments are shown in Fig. 6. With the increase of the initial concentration of Cu(II), Cd(II) and Cr(VI), the corresponding adsorption capacities of MgAl-LDH also gradually increased, which was consistent with the experimental results of Deng et al. [39]. Increasing the initial ion concentrations enhanced the

driving force between the body of solutions and particle surface concentrations, and provided to transcend the resistance to the mass transfer of metal ions on the interface, resulting in a higher adsorption capacity [40]. In the single adsorption systems with the initial concentration of Cu(II), Cd(II) and Cr(VI) of 10 mg/L, the removal efficiencies of Cu(II), Cd(II) and Cr(VI) reached adsorption equilibrium were close to 100%, 80% and 40%, respectively (Fig. 3). However, when the initial concentrations of Cu(II), Cd(II) and Cr(VI) were 150, 100, and 30 mg/L, respectively, the maximum adsorption capacities of MgAl-LDH for Cu(II), Cd(II) and Cr(VI) was 79.27, 63.62 and 11.30 mg/g, respectively. The corresponding heavy metal removal efficiencies were 26.42%, 31.81% and 18.83%, respectively, which showed that MgAl-LDH approximately reached saturate adsorption under this condition. In the study of Yue et al. [19], the addition of 2.0 g/L of Cl-LDH could altogether remove 40 mg/L of Cr(VI) in an aqueous solution containing single Cr(VI). As for a single Cr(VI) of 400 mg/L, the maximum adsorption capacity of Cl-LDH was 45.20 mg/g. The difference in adsorption efficiency might be because

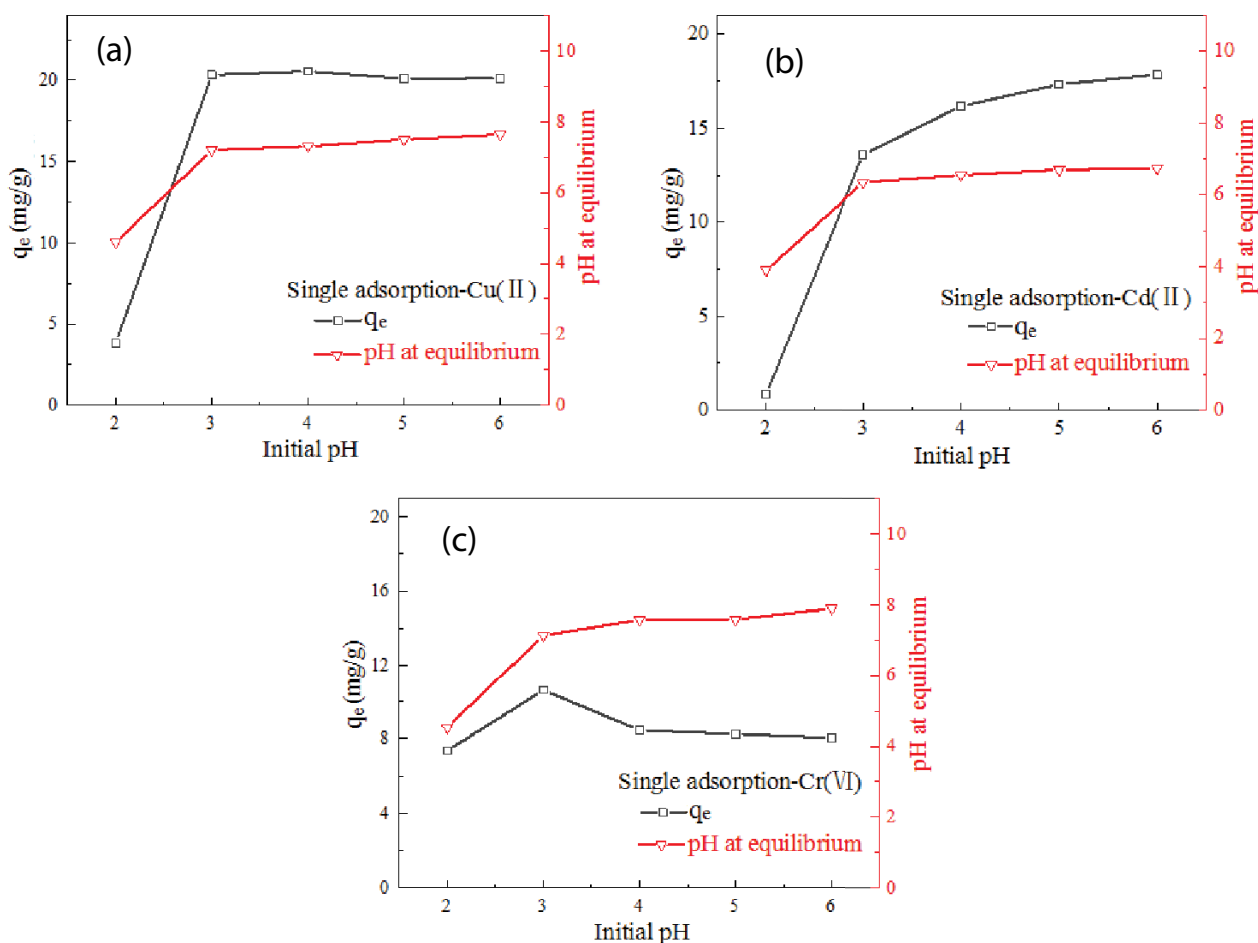


Fig. 4. Effect of initial pH value on the equilibrium adsorption capacity of (a) Cu(II), (b) Cd(II) and (c) Cr(VI) in single adsorption systems (Reaction temperature = 25°C; $m = 0.50$ g/L; $C_0 = 10$ mg/L; $V = 100$ mL).

they did not use Na_2CO_3 as an alkaline solution during the preparation of LDHs. Hence, the content of interlayer CO_3^{2-} and HCO_3^- in the LDHs prepared by them was less than the LDHs prepared in our experiment. Due to the strong affinity of CO_3^{2-} and HCO_3^- for the interlayer of LDHs, the anion exchange reaction between $\text{CO}_3^{2-}/\text{HCO}_3^-$ and Cr(VI) was very little [17,41]. In addition, the differences in temperature and the dosage of adsorbents might also be the reasons for the different adsorption capacities of LDHs.

3.2.3. Concentration of coexisting heavy metals

As shown in Fig. 7c, in the mixed system where the initial concentration of Cu(II) increased alone, Cu(II) took the lead in grabbing the adsorption sites in the adsorption process. The removal efficiency of Cd(II) dropped sharply from 72.06% to almost 0. However, the removal efficiency of Cr(VI) increased with the increase of initial Cu(II) concentration, and Cr(VI) could be removed entirely at the end of the reaction. The results might be because Cr(VI) appeared a rapid and effective ion exchange reaction with Cl^- in the interlayer of MgAl-LDH without adding Cu(II), resulting in a certain concentration of Cl^- existing in the solution, which promoted the stripping and dissolution

of the lamellar layers of MgAl-LDH. The dissolution of MgAl-LDH would cause immediate consumption of H_3O^+ and the release of abundant $-\text{OH}$ in the solution [19]. With the increase of Cu(II) concentration, Cu(II), Cl^- and some hydration-OH in the solution rapidly precipitated $\text{Cu}_2(\text{OH})_3\text{Cl}$, which was deposited on the surface of MgAl-LDH and occupied part of the adsorption sites. $\text{Cu}_2(\text{OH})_3\text{Cl}$ could remove Cr(VI) in solution by adsorption. The generation of $\text{Cu}_2(\text{OH})_3\text{Cl}$ consumed a large amount of $-\text{OH}$ in the solution, which induced a decrease in pH value in the system. As shown in Fig. 7a, the adsorption capacity of Cd(II) decreased with the increase of Cr(VI) concentration. In contrast, the adsorption capacity of Cu(II) did not change significantly and the removal efficiency of Cu(II) was close to 100%. The decrease in the equilibrium adsorption capacity of Cd(II) by MgAl-LDH might be since Cr(VI) and heavy metal cations would compete for the adsorption sites (i.e., the surface hydroxyl) on the LDH [37]. As shown in Fig. 7b, when the initial concentration of Cd(II) increased alone, the removal efficiency of Cu(II) was always close to 100%, and the removal efficiency of Cr(VI) slightly improved. The ionic radii of Cd^{2+} and Cu^{2+} were 0.095 nm and 0.073 nm, which were close to Mg^{2+} (0.066 nm). Hence, Cd^{2+} and Cu^{2+} were easily isomorphic

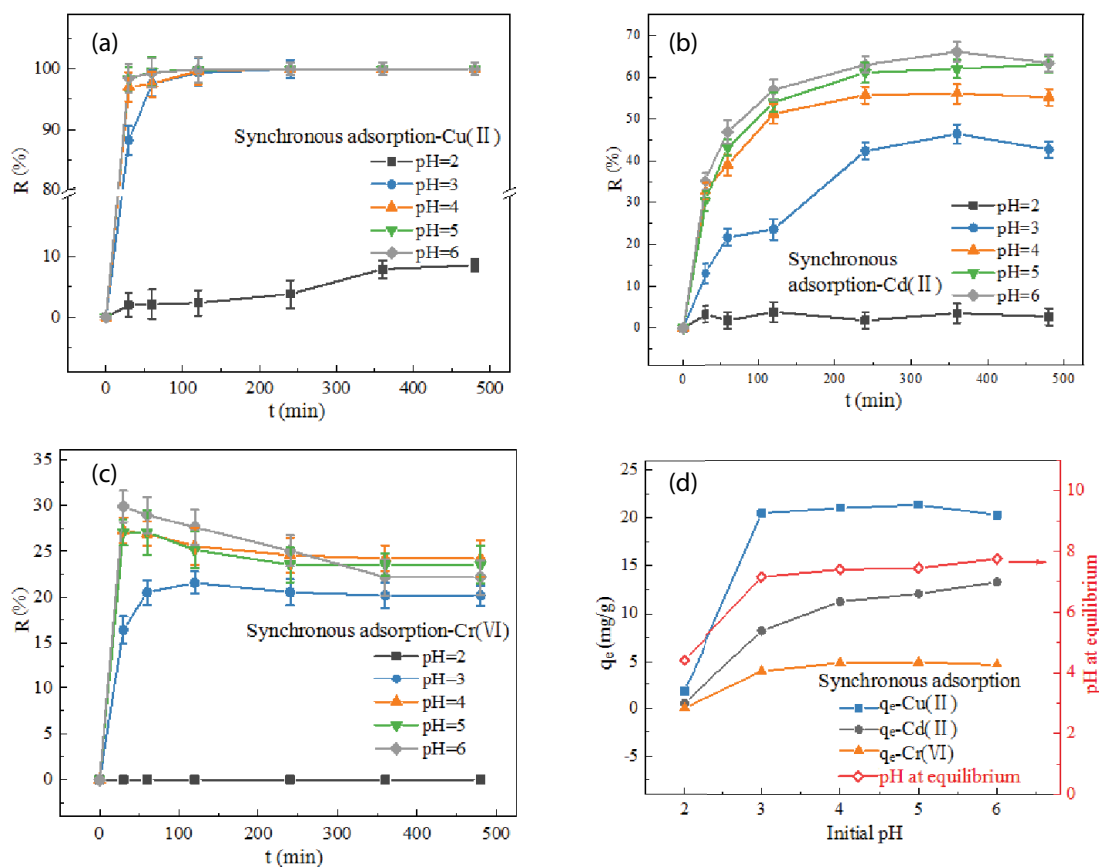


Fig. 5. Effect of initial pH value on the removal efficiency and equilibrium adsorption capacity of (a) Cu(II), (b) Cd(II) and (c) Cr(VI) in the synchronous adsorption system (Reaction temperature = 25°C; $m = 0.50$ g/L; $C_0 = 10$ mg/L; $V = 100$ mL).

to Mg^{2+} on the layers. Increasing Cd(II) concentration promoted more Cd^{2+} to replace Mg^{2+} on the laminates, which led to the enhancement of O–H acidity and the decrease of electrostatic repulsion between the adsorbents and anionic Cr(VI), and was conducive to the removal of Cr(VI).

3.2.4. Coexisting anions

There are usually a variety of anions in industrial effluents, and these coexisting anions may compete with Cr(VI) for adsorption, thus affecting the adsorption effect of MgAl-LDH on Cr(VI). The successful adsorption of Cr(VI) and F^- by MgAl-LDH showed that the binding force of Cr(VI) and F^- to the MgAl-LDH laminates was stronger than that of Cl^- . Moreover, competitive adsorption of Cr(VI) and F^- on MgAl-LDH occurred, and the adsorption affinity of MgAl-LDH for Cr(VI) was greater than that of F^- [42]. There are strong covalent bonds on the LDH layers, combined with interlayer anions through electrostatic interactions, hydrogen bonds, and van der Waals forces. Covalent bonds are highly selective and irreversible and are not affected by coexisting anions. The adsorption of anions by LDHs can be divided into interlayer anion exchange and external surface adsorption, which belong to weak interaction forces and are non-selective and reversible. Different coexisting anions

make LDHs exhibit different Cr(VI) adsorption capacities due to the competition for adsorption sites on the outer surface and the relative difference in electrostatic affinity in the interlayer. Combined with the findings of this experiment and related literature reports, the order of the interference of coexisting anions in the solution on the adsorption of Cr(VI) by MgAl-LDH was $CO_3^{2-} > HCO_3^- > F^- > Cl^-$ [17].

3.3. Adsorption kinetics and isotherms

3.3.1. Adsorption kinetics

In Fig. 8, the adsorption rates of Cu(II), Cd(II) and Cr(VI) by MgAl-LDH were faster within 100 min. As time went by, the reaction rate gradually decreased until the adsorption reached equilibrium. When the adsorbent was just added, the concentration of heavy metal ions was relatively high, and most of the adsorption sites on MgAl-LDH were not occupied. As the process progressed, the adsorption sites were gradually occupied, and the concentration of heavy metal ions decreased. The synchronous adsorption rate of Cu(II) was slightly faster than the single adsorption rate, but the synchronous adsorption rate of Cd(II) and Cr(VI) was somewhat slower than the single adsorption rate. To further explore the adsorption process, pseudo-first-order and pseudo-second-order kinetic models were used to conduct kinetic analysis on the experimental results of

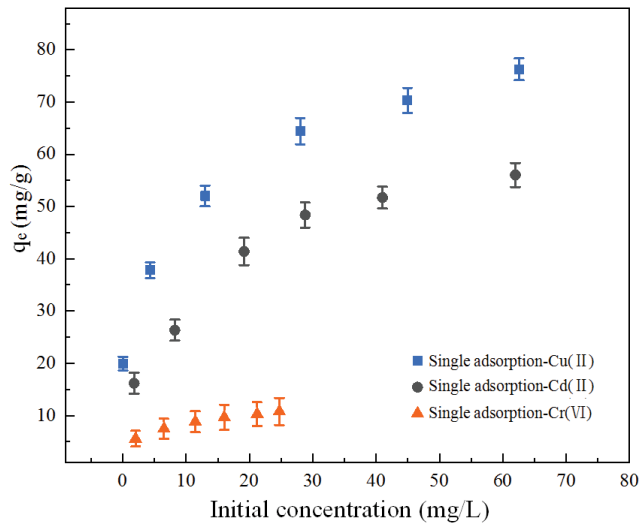


Fig. 6. Effect of initial solution concentration on the adsorption capacity of Cu(II), Cd(II) and Cr(VI) in single adsorption systems (Reaction temperature = 25°C; initial pH = 4; $m = 0.50$ g/L; $V = 100$ mL).

the single/synchronous adsorption systems, respectively, as shown in Fig. 8, and the kinetic parameters are shown in Table 1. The calculation formulas of pseudo-first-order and pseudo-second-order kinetic models are as follows:

$$q_t = q_e (1 - e^{-k_1 t}) \tag{3}$$

$$q_t = \frac{k_2 q_e^2 t}{1 + k_2 q_e t} \tag{4}$$

where q_t and q_e (mg/g) are the adsorption capacities at time t and equilibrium, respectively; k_1 (min^{-1}) and k_2 (g/mg min) are pseudo-first-order and pseudo-second-order rate constants, respectively.

Comparing the parameters of pseudo-first-order and pseudo-second-order kinetic models, it could be seen that the R^2 of the pseudo-second-order kinetic model was greater than that of the pseudo-first-order, indicating that the adsorption kinetics model of MgAl-LDH for Cu(II), Cd(II) and Cr(VI) was more consistent with a pseudo-second-order kinetic model.

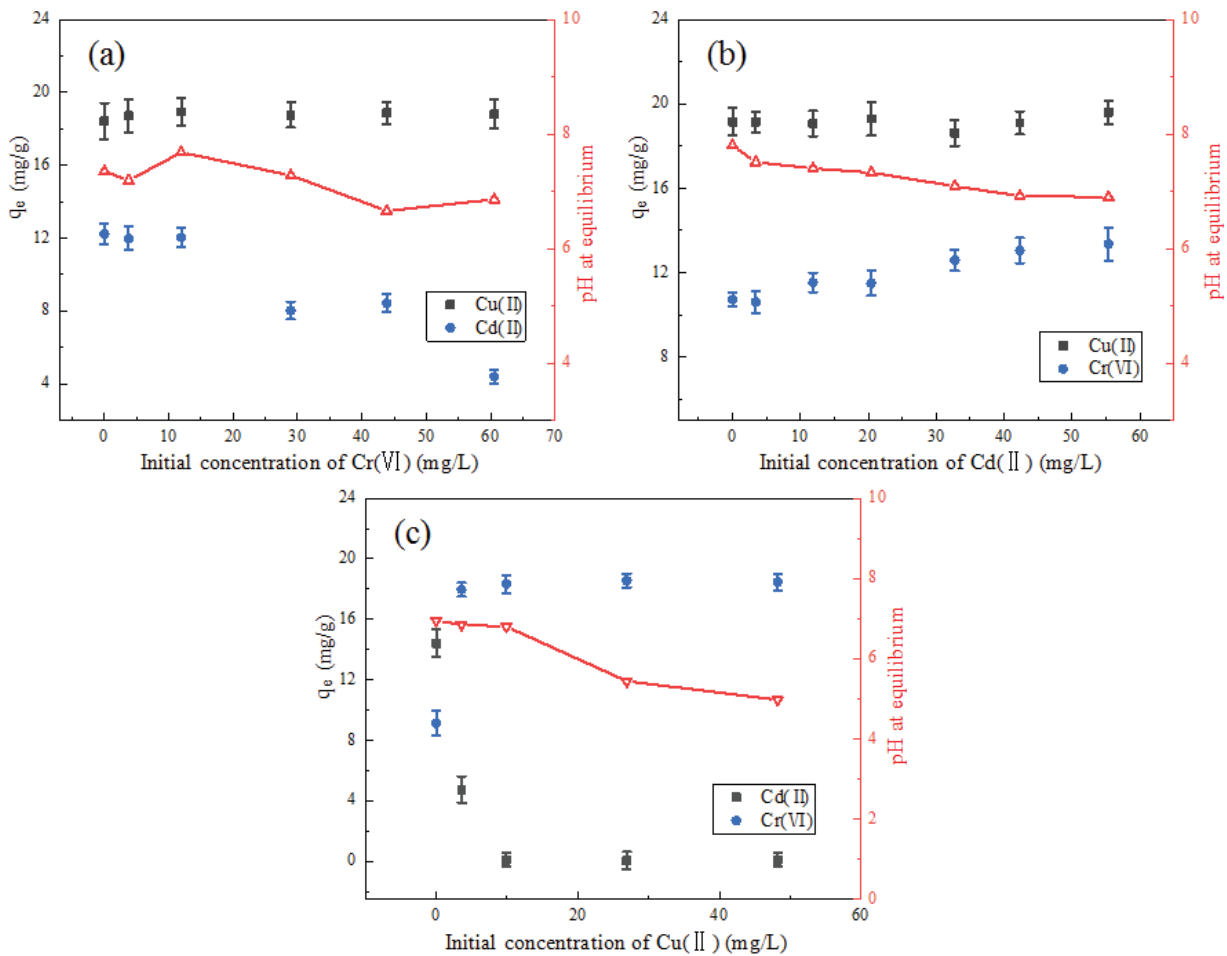


Fig. 7. Effect of initial concentration of (a) Cr(VI), (b) Cd(II) and (c) Cu(II) on the synchronous adsorption performance of MgAl-LDH (Reaction temperature = 25°C; initial pH = 4; $m = 0.50$ g/L; $V = 50$ mL).

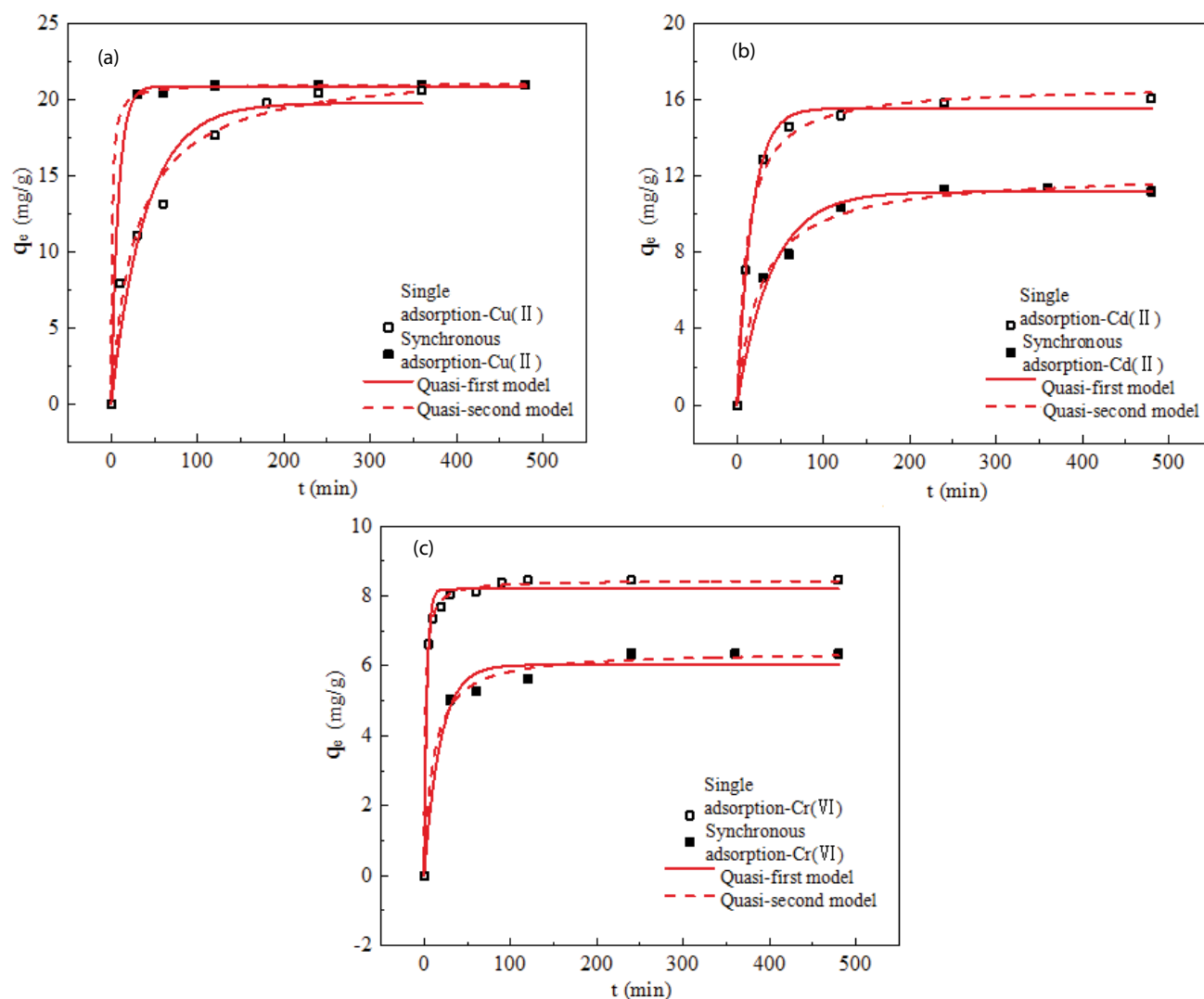


Fig. 8. Adsorption kinetics of the removal of (a) Cu(II), (b) Cd(II) and (c) Cr(VI) by MgAl-LDH in the single/synchronous adsorption system (Reaction temperature = 25°C; initial pH = 4; $m = 0.50$ g/L; $C_0 = 10$ mg/L; $V = 50$ mL).

Table 1
Kinetic parameters of Cu(II), Cd(II) and Cr(VI) adsorption on MgAl-LDH

Sample	Quasi-first-model parameters			Quasi-second-model parameters		
	k_1 (min^{-1})	q_e (mg/g)	R^2	k_2 ((g/mg)/min)	q_e (mg/g)	R^2
Single adsorption-Cu(II)	0.077	19.589	0.999	0.014	20.010	0.999
Single adsorption-Cd(II)	0.280	19.883	0.999	0.065	20.081	0.999
Single adsorption-Cr(VI)	0.279	8.201	0.998	0.141	8.310	0.999
Synchronous adsorption-Cu(II)	0.066	19.436	0.999	0.010	19.638	0.999
Synchronous adsorption-Cd(II)	0.019	16.266	0.979	0.001	18.216	0.995
Synchronous adsorption-Cr(VI)	0.081	5.335	0.976	0.142	5.327	0.979

3.3.2. Adsorption isotherms

Adsorption isotherms can reflect the relationship between equilibrium concentration and equilibrium adsorption capacity and are essential parameters to analyze the

adsorption capacity of adsorbents. In this article, Langmuir and Freundlich's adsorption isotherm models were used to fit the experimental data of MgAl-LDH separately adsorbing Cu(II), Cd(II) and Cr(VI). Fitting results are shown in Fig. 9 and Table 2. The calculation formulas of

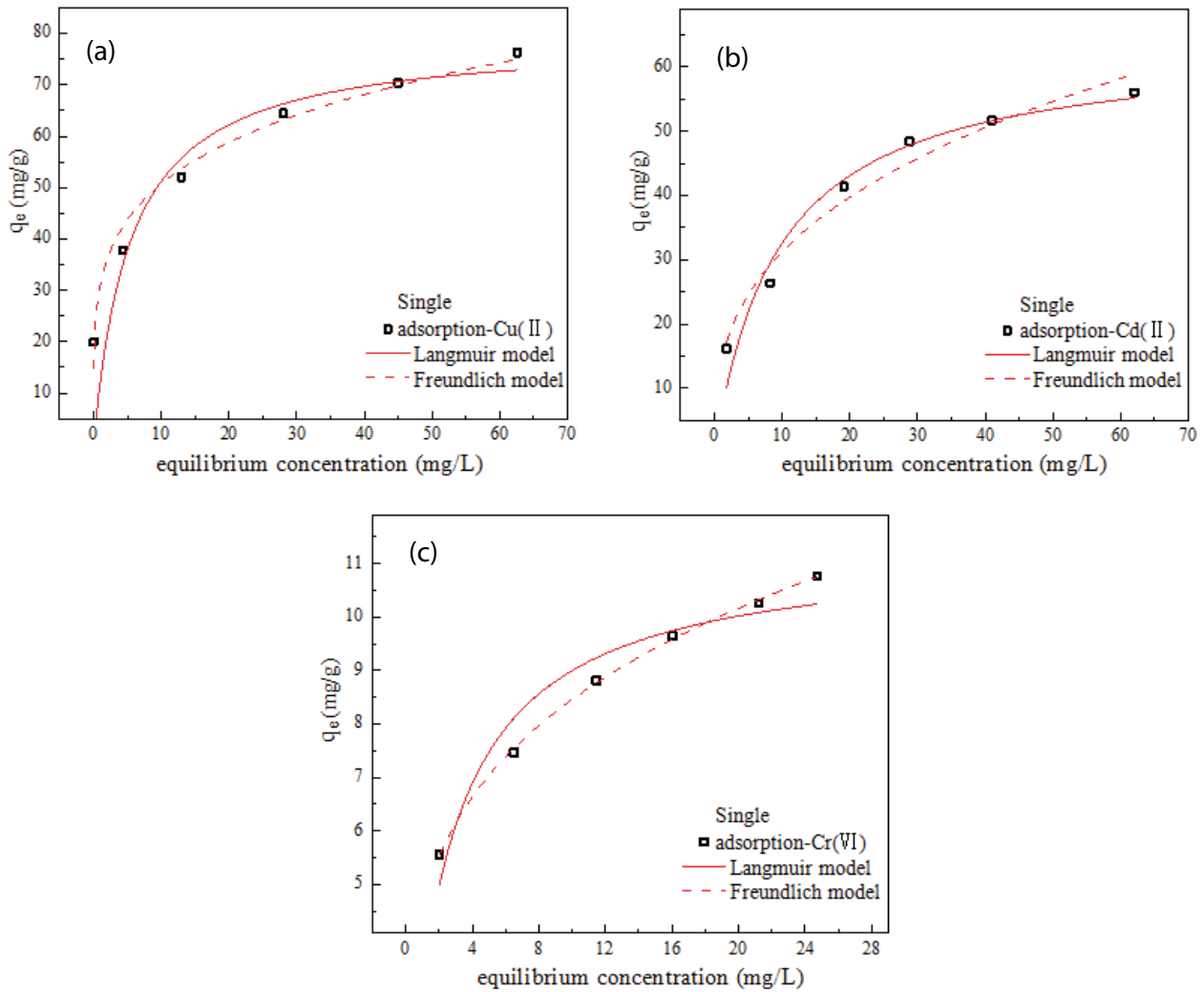


Fig. 9. Adsorption isotherms of (a) Cu(II), (b) Cd(II) and (c) Cr(VI) removed by MgAl-LDH (Reaction temperature = 25°C; initial pH = 4; $m = 0.50$ g/L; $V = 50$ mL).

Table 2
Isotherm parameters of adsorption of Cu(II), Cd(II) and Cr(VI) by MgAl-LDH

Sample	Langmuir parameters			Freundlich parameters		
	q_m (mg/g)	b (L/mg)	R^2	K_F ((mg/g)/(mg/L) ^{n})	$1/n$	R^2
Cu(II)	79.271	0.183	0.818	31.074	0.213	0.976
Cd(II)	63.617	0.105	0.960	14.046	0.347	0.973
Cr(VI)	11.299	0.391	0.935	4.600	0.265	0.999

Langmuir and Freundlich adsorption isotherm models are as follows:

$$q_e = \frac{q_m b C_e}{1 + b C_e} \tag{5}$$

$$q_e = K_F C_e^{1/n} \tag{6}$$

where q_e and q_m (mg/g) are the adsorption capacity at adsorption equilibrium and the maximum adsorption capacity of the adsorbent, respectively; C_e (mg/L) is the equilibrium concentration of the adsorbates; b is the Langmuir model constant related to the adsorption energy; K_F and n are Freundlich model constants, where n is the adsorption strength index.

R^2 of the Freundlich model was higher than that of the Langmuir model. Therefore, the adsorption processes of Cu(II), Cd(II) and Cr(VI) by MgAl-LDH were more in line

with the Freundlich adsorption isotherm, which showed that the surface of MgAl-LDH had different active adsorption sites and the adsorption of Cu(II), Cd(II) and Cr(VI) was heterogeneous [43]. In the Freundlich model, the $1/n$ values of Cu(II), Cd(II) and Cr(VI) were between 0.1 and 0.5, indicating that the adsorption was easy to proceed with the study of Ho et al. [44]. The adsorption processes of Cu(II), Cd(II) and Cr(VI) by MgAl-LDH included both physical adsorption and chemical adsorption.

3.4. Mechanisms

The XRD pattern is shown in Fig. 10. There was no apparent miscellaneous peak in the XRD pattern, indicating that the crystallinity of the material was good. There were prominent characteristic peaks at 11.16° , 22.56° , 34.45° , 38.51° , 60.26° and 61.45° at 2θ . These peaks were judged to be consistent with the typical characteristic peaks (003), (006), (012), (015), (110) and (113) of layered hydroxides, corresponding to the JCPDS card number 35-0965 in PDF card. In Table 3, after adsorption of Cr(VI),

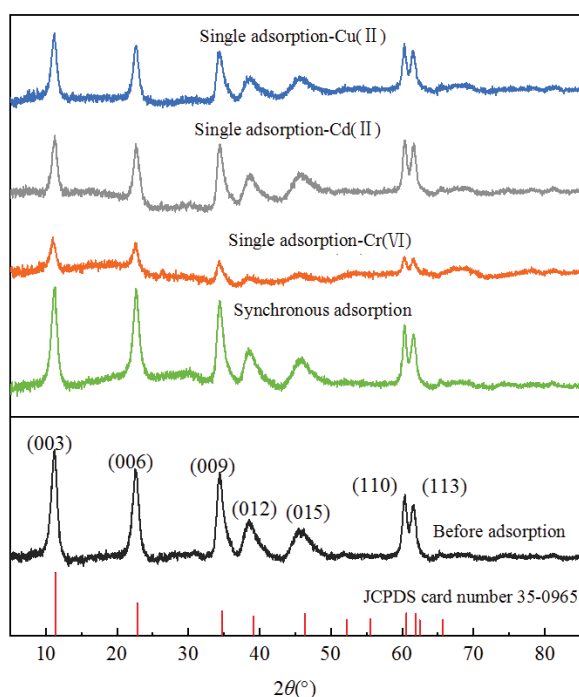


Fig. 10. XRD spectra of MgAl-LDH before and after adsorption.

the interlayer spacing increased from 0.788 to 0.797 nm and the diffraction peaks of the sample became broader and less intense, indicating that the anion exchange reaction occurred between Cr(VI) and interlayer anions [30], which enlarged the gallery height for the larger ionic size of Cr(VI) anions. Generally, the smaller the radius of the replacement anion and the negative charge capacity, the greater the replacement performance [45].

As shown in the FTIR spectra (Fig. 11), the broad bands at 3461 and 1636 cm^{-1} were associated with the stretching vibrations of the OH group in the brucite-like layers and bending vibration of water molecules in the interlayer. The band at 1384 cm^{-1} was due to the vibration mode of CO_3^{2-} that might be introduced into the interlayer of MgAl-LDH by absorption of CO_2 during the preparation procedure [30]. The bands between 400 and 800 cm^{-1} were attributed to the characteristic lattice vibrations of MgO and Al_2O_3 . In addition, a weak band at 880 cm^{-1} was also observed in the spectra of Cr(VI) adsorption alone and synchronous adsorption. The band was the characteristic infrared band of chromate

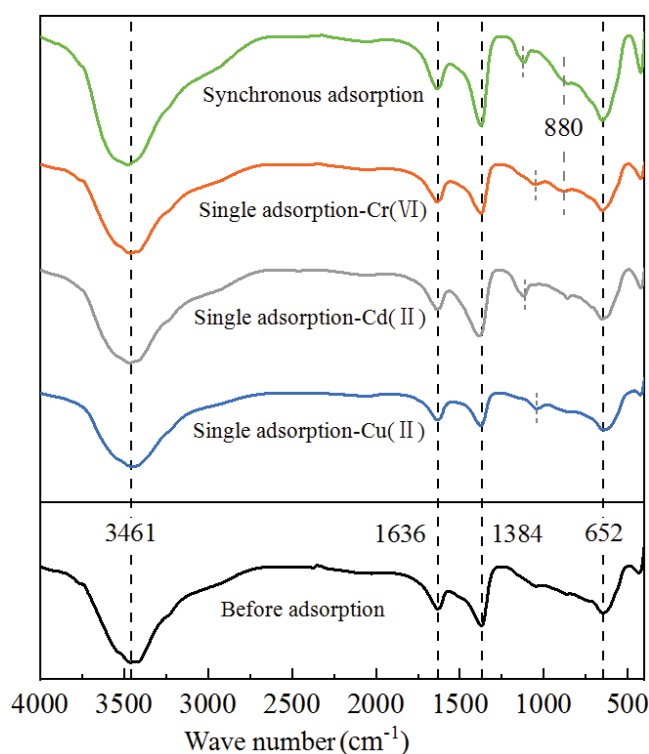


Fig. 11. FTIR spectra before and after MgAl-LDH adsorption.

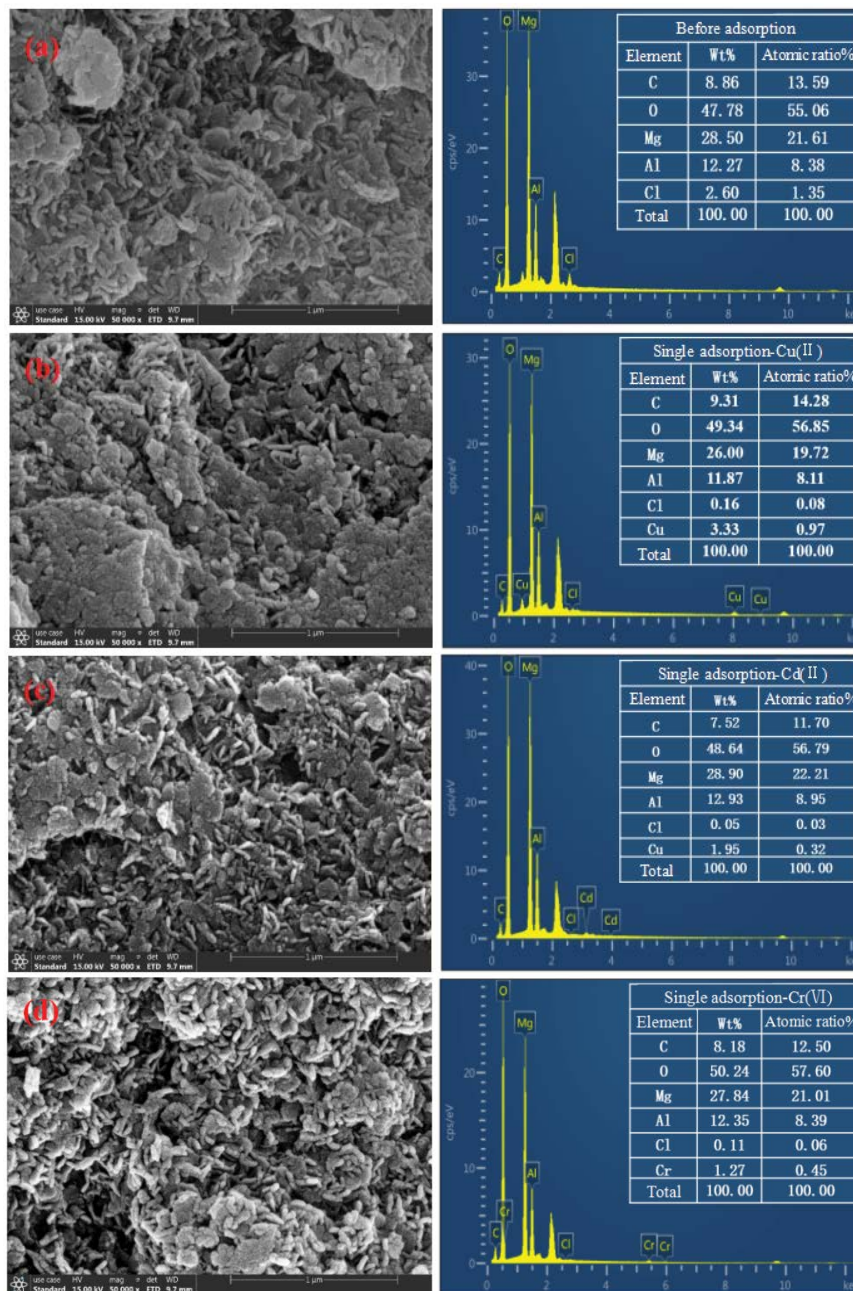
Table 3
XRD lattice parameters

Sample	Basic spacing (nm)	Lattice parameter a (nm)	Lattice parameter c (nm)
Before adsorption	0.788	0.306	2.364
After adsorption of Cu(II)	0.787	0.307	2.360
After adsorption of Cd(II)	0.786	0.306	2.357
After adsorption of Cr(VI)	0.797	0.307	2.392
After synchronous adsorption	0.787	0.307	2.361

corresponding to mode ν_d (Cr–O), which was recorded at 890 cm^{-1} for free chromate. A relative slight shift towards lower frequency might be due to the hydrogen bonding of Cr(VI) anion with interlayer water molecules or layer hydroxyl groups.

The SEM-EDS spectrum is shown in Fig. 12. The MgAl-LDH prepared had a uniform structure, a typical hexagonal layered structure of hydroxyl materials, and a porous surface with many pores, which increased the adsorption space and was conducive to the adsorption. It could be seen from the EDS spectrum that Cu(II), Cd(II) and Cr(VI) were detected, indicating that the three ions were successfully adsorbed. Furthermore, some small particles were attached to the sample's surface after adsorbing Cu(II)

alone, and the agglomeration phenomenon was significant, which might be that the $\text{Cu}_2(\text{OH})_3\text{Cl}$ precipitate formed during the adsorption process was deposited on the sample. The molar ratios of Mg/Al changed from 2.58:1 before adsorption to 2.43:1, 2.48:1, 2.55:1, 2.33:1, respectively, indicating that Cd^{2+} and Cu^{2+} underwent isomorphous substitution with Mg^{2+} on the layers, and $(\text{M}^{2+}\text{Mg})_2\text{Al}(\text{OH})_6\text{Cl}$ was obtained after recombination. Yue et al. [19] found that the distribution of element Cu was consistent with the basic distribution of element Mg in the result of element mapping of Cl-LDH-CuCr, again confirming this conclusion. The atomic percentage of Cl decreased from 1.35 before adsorption to 0.08, 0.03, 0.06 and 0.04 after adsorption, respectively, indicating that anion exchange occurred between



(Continued)

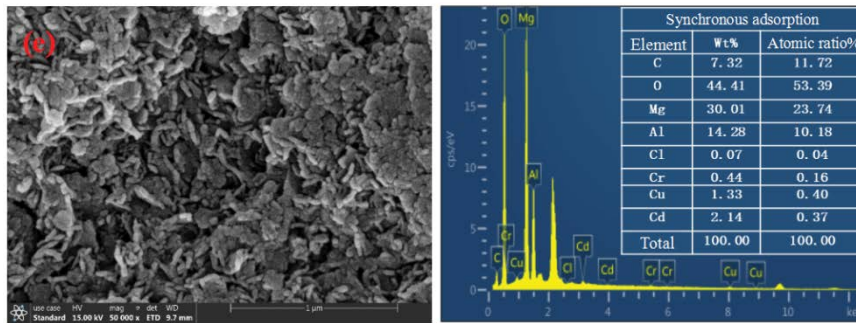


Fig. 12. SEM and EDS images before and after MgAl-LDH adsorption ((a) before adsorption, (b) single adsorption-Cu(II), (c) single adsorption-Cd(II), (d) single adsorption-Cr(VI) and (e) synchronous adsorption).

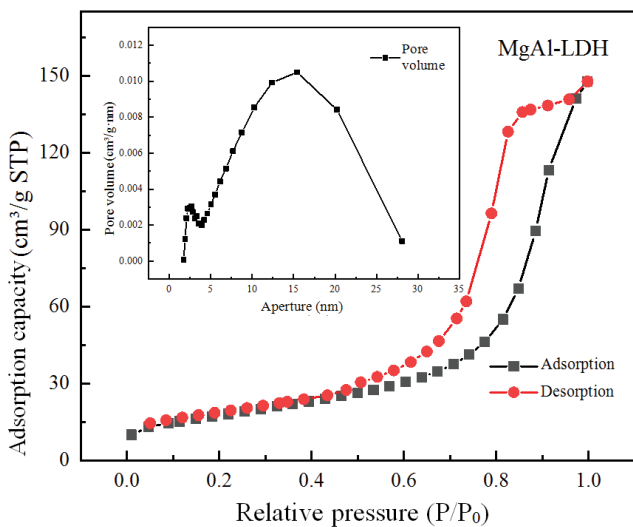


Fig. 13. N₂ adsorption/desorption isotherm and pore-size distribution of MgAl-LDH.

CrO₄²⁻ and Cl⁻. In addition, it could be seen from the SEM images that part of the structure had collapsed after adsorption, so the stability of MgAl-LDH needed to be further improved.

The N₂ adsorption–desorption curve and pore-size distribution of MgAl-LDH are shown in Fig. 13. The specific surface area of the prepared sample was 63.41 m²/g. Generally, the larger the specific surface area was, the larger the adsorption capacity of the adsorbent would be. This isotherm belonged to the IV type N₂ adsorption–desorption curve, H1 hysteresis loop in the IUPAC classification. The average pore size of MgAl-LDH was 13.20 nm, which belonged to mesoporous (2–50 nm). It could be seen that adsorption capacity increased gently in the low-pressure section ($P/P_0 = 0.0-0.1$), and there was a sudden increase in adsorption capacity around $P/P_0 = 0.5-0.8$. In summary, MgAl-LDH was an ordered mesoporous material.

Based on all the above analyses, possible mechanisms of removing Cu(II), Cd(II) and Cr(VI) by MgAl-LDH were proposed, as illustrated in Fig. 14.

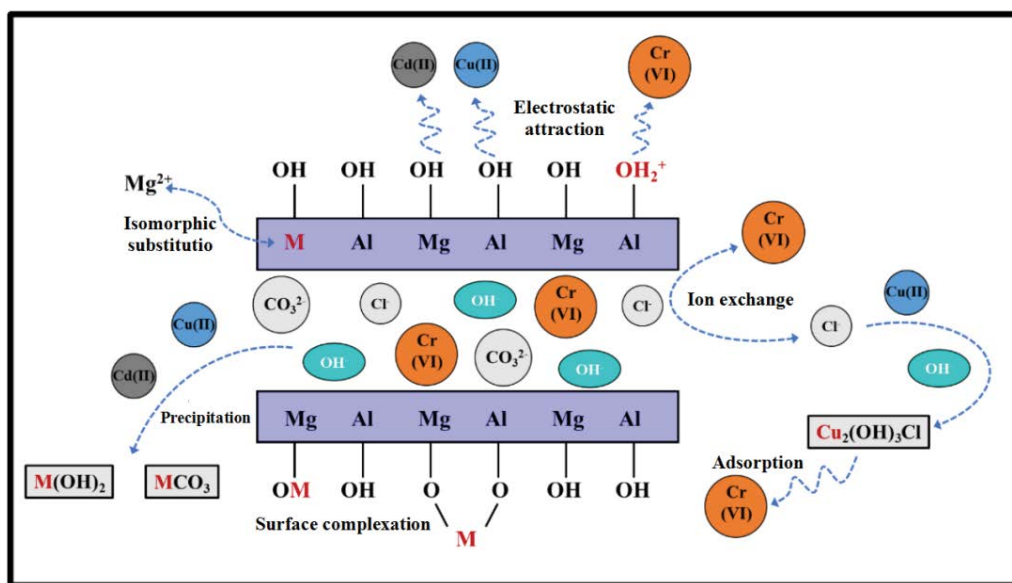


Fig. 14. Mechanism diagram of removing Cu(II), Cd(II) and Cr(VI) by MgAl-LDH (M = Cu(II), Cd(II)).

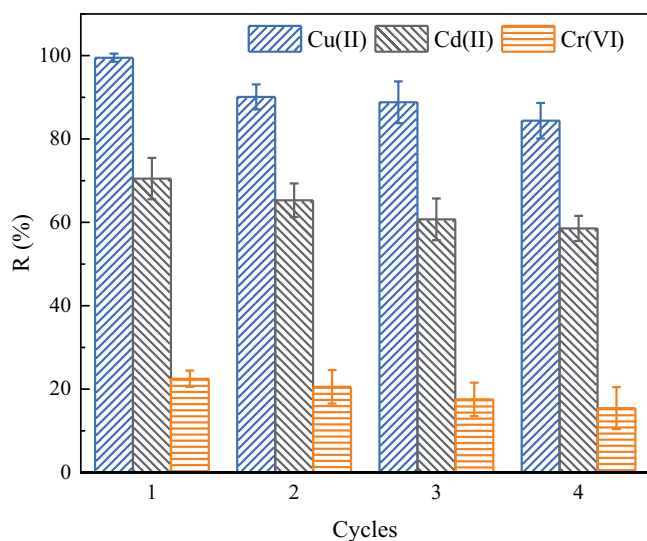


Fig. 15. Effect of cycles of MgAl-LDH on removal efficiencies of Cu(II), Cd(II) and Cr(VI) in the synchronous adsorption system (Reaction temperature = 25°C; initial pH = 4; C_0 = 10 mg/L; V = 100 mL).

3.5. Reusability of the adsorbent

The reusability of adsorbents is one of the critical factors to determine whether they can be put into practical engineering applications. In this study, MgAl-LDH after synchronous adsorption was placed in a certain amount of desorption solution, and the mixture was magnetically stirred at room temperature for 8 h. Then the desorption solution on the surface was rinsed after filtration. The desorbed MgAl-LDH was placed in a mixed solution of Cu(II), Cd(II) and Cr(VI) at 10 mg/L each to test the reusability of the adsorbent. Fig. 15 shows the synchronous adsorption removal efficiencies of the adsorbent after being reused four times. In the first cycle, the removal efficiencies of MgAl-LDH for Cu(II), Cd(II) and Cr(VI) reached 99.50%, 70.28% and 22.50%, respectively. After four cycles, the removal efficiencies were 84.39%, 58.55% and 15.43%, respectively, indicating that MgAl-LDH still maintained good adsorption performance. In addition, MgAl-LDH could be quickly separated by filtration, and maintained its complete morphology after multiple cycles without structural damage, indicating that the prepared MgAl-LDH had good mechanical strength and was suitable for practical applications.

4. Conclusion

Four types of MAI-LDH ($M = \text{Mg, Zn, Co, Ca}$) materials doped with different divalent metals were prepared by the co-precipitation method, and their adsorption performance for Cu(II), Cd(II) and Cr(VI) in the single/synchronous adsorption systems were compared. Among them, MgAl-LDH showed the best comprehensive adsorption performance and the highest stability. The optimal dosage of MgAl-LDH for Cu(II), Cd(II) and Cr(VI) adsorption was 0.50 g/L, and the optimal initial pH was 4. In general, the adsorption capacities of MgAl-LDH increased with the increase in the initial concentrations of the corresponding heavy metal solutions.

The affinity of MgAl-LDH to Cu(II) was more potent than that of Cd(II). The increase of Cu(II) concentration could promote the removal of Cr(VI). The adsorption behavior of MgAl-LDH on Cu(II), Cd(II) and Cr(VI) accorded with the pseudo-second-order kinetic model and Freundlich isotherm model. Combined with the characterization results, we proposed that MgAl-LDH removed Cu(II) and Cd(II) by electrostatic adsorption, surface complexation, precipitation and isostructural substitution, and removed Cr(VI) by external surface adsorption, interlayer anion exchange and $\text{Cu}_2(\text{OH})_3\text{Cl}$ precipitation adsorption. Additionally, MgAl-LDH had good reusability for synchronous adsorption so that it could be extended to practical applications.

Acknowledgement

This research was supported by the International Scientific and Technological Innovation and Cooperation Project of Sichuan (No. 2019YFH0170).

References

- [1] J. Hahladakis, E. Smaragdaki, G. Vasilaki, E. Gidaracos, Use of sediment quality guidelines and pollution indicators for the assessment of heavy metal and PAH contamination in Greek surficial sea and lake sediments, *Environ. Monit. Assess.*, 185 (2013) 2843–2853.
- [2] P. Zito, H.J. Shipley, Inorganic nano-adsorbents for the removal of heavy metals and arsenic: a review, *RSC Adv.*, 5 (2015) 29885–29907.
- [3] I. Ali, O.M.L. Alharbi, Z.A. Allothman, A.Y. Badjah, Kinetics, thermodynamics, and modeling of amido black dye photodegradation in water using Co/TiO₂ nanoparticles, *Photochem. Photobiol.*, 94 (2018) 935–941.
- [4] B.Y. Tu, R.T. Wen, K.Q. Wang, Y.L. Cheng, Y.Q. Deng, W. Cao, K.H. Zhang, H.S. Tao, Efficient removal of aqueous hexavalent chromium by activated carbon derived from Bermuda grass, *J. Colloid Interface Sci.*, 560 (2020) 649–658.
- [5] V. Mario, N.E.-Q. Ingrid, S.-C. Carlos, The influence of particle size and structure on the sorption and oxidation behavior of bismessite: I. Adsorption of As(V) and oxidation of As(III), *Geochim. Cosmochim. Acta*, 125 (2014) 564–581.
- [6] S.Y. Lee, S.J. Kim, Adsorption of naphthalene by HDTMA modified kaolinite and halloysite, *Appl. Clay Sci.*, 22 (2002) 55–63.
- [7] F.L. Fu, Q. Wang, Removal of heavy metal ions from wastewaters: a review, *J. Environ. Manage.*, 92 (2011) 407–418.
- [8] S. Santos, G. Ungureanu, B. Rui, C. Botelho, Selenium contaminated waters: an overview of analytical methods, treatment options and recent advances in sorption methods, *Sci. Total Environ.*, 521–522 (2015) 246–260.
- [9] D. Mohan, C.U. Pittman Jr., Arsenic removal from water/wastewater using adsorbents—a critical review, *J. Hazard. Mater.*, 142 (2007) 1–53.
- [10] X.Y. Yuan, Y.F. Wang, J. Wang, C. Zhou, Q. Tang, X.B. Rao, Calcined graphene/MgAl-layered double hydroxides for enhanced Cr(VI) removal, *Chem. Eng. J.*, 221 (2013) 204–213.
- [11] S.F. Zhao, M. Wu, R.S. Jing, X.J. Liu, Y.F. Shao, Q. Zhang, F.Z. Lv, A.J. Liu, Z.L. Meng, One-pot formation of magnetic layered double hydroxide based on electrostatic self-assembly to remove Cr(VI) from wastewater, *Appl. Clay Sci.*, 182 (2019) 105297, doi: 10.1016/j.clay.2019.105297.
- [12] Y.J. Lin, Q. Fang, B.L. Chen, Metal composition of layered double hydroxides (LDHs) regulating ClO₄⁻ adsorption to calcined LDHs via the memory effect and hydrogen bonding, *J. Environ. Sci.*, 26 (2014) 493–501.
- [13] G. Fan, F. Li, D.G. Evans, X. Duan, Catalytic applications of layered double hydroxides: recent advances and perspectives, *Chem. Soc. Rev.*, 43 (2014) 7040–7066.

- [14] S. Miyata, T. Kumura, Synthesis of new hydrotalcite-like compounds and their physico-chemical properties, *Chem. Lett.*, 2 (1973) 843–848.
- [15] X. Zhang, R.R. Shan, X.G. Li, L.G. Yan, Z.M. Ma, R.B. Jia, S.H. Sun, Effective removal of Cu(II), Pb(II) and Cd(II) by sodium alginate intercalated MgAl-layered double hydroxide: adsorption properties and mechanistic studies, *Water Sci. Technol.*, 83 (2021) 975–984.
- [16] H. Azad, M. Mohsenia, A novel free-standing polyvinyl butyral-polyacrylonitrile/ZnAl-layered double hydroxide nanocomposite membrane for enhanced heavy metal removal from wastewater, *J. Membr. Sci.*, 615 (2020) 118487, doi: 10.1016/j.memsci.2020.118487.
- [17] W.W. Wang, J.B. Zhou, G. Achari, J.G. Yu, W.Q. Cai, Cr(VI) removal from aqueous solutions by hydrothermal synthetic layered double hydroxides: adsorption performance, coexisting anions and regeneration studies, *Colloids Surf., A*, 457 (2014) 33–40.
- [18] T. Kameda, E. Kondo, T. Yoshioka, Treatment of Cr(VI) in aqueous solution by Ni–Al and Co–Al layered double hydroxides: equilibrium and kinetic studies, *J. Water Process Eng.*, 8 (2015) e75–e80.
- [19] X.Y. Yue, W.Z. Liu, Z.L. Chen, Z. Lin, Simultaneous removal of Cu(II) and Cr(VI) by Mg–Al–Cl layered double hydroxide and mechanistic insight, *J. Environ. Sci.*, 53 (2017) 16–26.
- [20] J.L. Milagres, C.R. Bellato, R.S. Vieira, S.O. Ferreira, C. Reis, Preparation and evaluation of the Ca–Al layered double hydroxide for removal of copper(II), nickel(II), zinc(II), chromium(VI) and phosphate from aqueous solutions, *J. Environ. Chem. Eng.*, 5 (2017) 5469–5480.
- [21] M.A. González, I. Pavlovic, C. Barriga, Cu(II), Pb(II) and Cd(II) sorption on different layered double hydroxides. A kinetic and thermodynamic study and competing factors, *Chem. Eng. J.*, 269 (2015) 221–228.
- [22] H. Yan, M. Wei, J. Ma, F. Li, D.G. Evans, X. Duan, Theoretical study on the structural properties and relative stability of M(II)–Al layered double hydroxides based on a cluster model, *J. Phys. Chem. A*, 113 (2009) 6133–6141.
- [23] L. Li, A Novel Method for the Synthesis of Hydrotalcites and A Theoretical Study of Their Structure and Properties, Beijing University of Chemical Technology, China, 2002.
- [24] S.P. Dubey, K. Gopal, Adsorption of chromium(VI) on low cost adsorbents derived from agricultural waste material: a comparative study, *J. Hazard. Mater.*, 145 (2007) 465–470.
- [25] M.N. Mohamad Ibrahim, W.S. Wan Ngah, M.S. Norliyana, W.R. Wan Daud, M. Rafatullah, O. Sulaiman, R. Hashim, A novel agricultural waste adsorbent for the removal of lead(II) ions from aqueous solutions, *J. Hazard. Mater.*, 182 (2010) 377–385.
- [26] Y.-B. Zang, W.-G. Hou, W.-X. Wang, Adsorption–desorption of chromium(VI) on Mg–Al hydrotalcite-like compounds part I. Adsorption, *Acta Chim. Sinica – Chinese Edition*, 65 (2007) 773–778.
- [27] S. Mor, K. Ravindra, N.R. Bishnoi, Adsorption of chromium from aqueous solution by activated alumina and activated charcoal, *Bioresour. Technol.*, 98 (2007) 954–957.
- [28] L. Qin, L. Yan, J. Chen, T. Liu, H. Yu, B. Du, Enhanced removal of Pb²⁺, Cu²⁺, and Cd²⁺ by amino-functionalized magnetite/kaolin clay, *Ind. Eng. Chem. Res.*, 55 (2016) 7344–7354.
- [29] X.F. Liang, Y.B. Zang, Y.M. Xu, X. Tan, W. Hou, L. Wang, Y.B. Sun, Sorption of metal cations on layered double hydroxides, *Colloids Surf., A*, 433 (2013) 122–131.
- [30] Y.J. Li, B.Y. Gao, T. Wu, D.J. Sun, X. Li, B. Wang, F.J. Lu, Hexavalent chromium removal from aqueous solution by adsorption on aluminum magnesium mixed hydroxide, *Water Res.*, 43 (2009) 3067–3075.
- [31] N.N. Wang, A.H. Wang, L.H. Kong, M.C. He, Calculation and application of Sb toxicity coefficient for potential ecological risk assessment, *Sci. Total Environ.*, 610–611 (2017) 167–174.
- [32] L.-n. Shi, X. Zhang, Z.-l. Chen, Removal of chromium(VI) from wastewater using bentonite-supported nanoscale zero-valent iron, *Water Res.*, 45 (2011) 886–892.
- [33] Y.L. Xu, J.Y. Chen, R. Chen, P.L. Yu, S. Guo, X.F. Wang, Adsorption and reduction of chromium(VI) from aqueous solution using polypyrrole/calcium rectorite composite adsorbent, *Water Res.*, 160 (2019) 148–157.
- [34] Z.F. Yu, W.F. Song, J.Y. Li, Q.H. Li, Improved simultaneous adsorption of Cu(II) and Cr(VI) of organic modified metakaolin-based geopolymer, *Arabian J. Chem.*, 13 (2020) 4811–4823.
- [35] F.L. Ling, L. Fang, Y. Lu, J.M. Gao, F. Wu, M. Zhou, B. Hu, A novel CoFe layered double hydroxides adsorbent: high adsorption amount for methyl orange dye and fast removal of Cr(VI), *Microporous Mesoporous Mater.*, 234 (2016) 230–238.
- [36] R.L. Goswamee, P. Sengupta, K.G. Bhattacharyya, D.K. Dutta, Adsorption of Cr(VI) in layered double hydroxides, *Appl. Clay Sci.*, 13 (1998) 21–34.
- [37] M.W. Laipan, H.Y. Fu, R.L. Zhu, L.Y. Sun, M.S. Rachel, S. Ye, J.X. Zhu, H.P. He, Calcined Mg/Al-LDH for acidic wastewater treatment: simultaneous neutralization and contaminant removal, *Appl. Clay Sci.*, 153 (2018) 46–53.
- [38] T. Kameda, S. Saito, Y. Umetsu, Mg–Al layered double hydroxide intercalated with ethylene-diaminetetraacetate anion: synthesis and application to the uptake of heavy metal ions from an aqueous solution, *Sep. Purif. Technol.*, 47 (2005) 20–26.
- [39] L. Deng, Z. Shi, L. Wang, S.Q. Zhou, Fabrication of a novel NiFe₂O₄/Zn–Al layered double hydroxide intercalated with EDTA composite and its adsorption behavior for Cr(VI) from aqueous solution, *J. Phys. Chem. Solids*, 104 (2017) 79–90.
- [40] M. Alok, M. Jyoti, M. Arti, V.K. Gupta, Adsorptive removal of hazardous anionic dye “Congo red” from wastewater using waste materials and recovery by desorption, *J. Colloid Interface Sci.*, 340 (2009) 16–26.
- [41] A.V. Radha, P.V. Kamath, C. Shivakumara, Mechanism of the anion exchange reactions of the layered double hydroxides (LDHs) of Ca and Mg with Al, *Solid State Sci.*, 7 (2005) 1180–1187.
- [42] H. Wang, W. Liao, H.Q. Li, Simultaneous adsorption of Cr(VI) and fluoride from aqueous over multiple-metal layer double hydroxides: performance and mechanism, *Desal. Water Treat.*, 179 (2020) 197–210.
- [43] L. Peng, Study on Adsorption of Four Hydrotalcite Materials for Heavy Metal, Huazhong University of Science and Technology, China, 2018.
- [44] Y.S. Ho, J.C.Y. Ng, G. McKay, Kinetics of pollutant sorption by biosorbents: review, *Sep. Purif. Rev.*, 29 (2000) 189–232.
- [45] D.L. Huang, C.H. Liu, C. Zhang, R. Deng, R.Z. Wang, W.J. Xue, H. Luo, G.M. Zeng, Q. Zhang, X.Y. Guo, Cr(VI) removal from aqueous solution using biochar modified with Mg/Al-layered double hydroxide intercalated with ethylenediaminetetraacetic acid, *Bioresour. Technol.*, 276 (2018) 127–132.